# Ultrafine Particles Emitted Through Routine Operation of a Hairdryer

Joseph Nelson Dawson, Kristin E. DiMonte, Matthew J. Griffin, and Miriam Arak Freedman*

*Department of Chemistry, The Pennsylvania State University, University, PA 16802, United States*

*Revised Submission to Environmental Science and Technology*

*May 27, 2021*

## Abstract

Particulate matter is a large concern for human health. Fine and ultrafine particulate matter has been shown to negatively impact human health; such as, causing cardiopulmonary diseases. Current regulation targets the size of the particles, but composition also impacts toxicity. Indoor sources of air pollution pose unique challenges for human health due to the potential for human exposure to high concentrations in confined spaces. In this work, six hairdryers were each operated within a plexiglass chamber, and their emissions were analyzed with transmission electron microscopy and energy dispersive spectroscopy (EDS). All hairdryers were found to emit ultrafine iron, carbon, and copper. In addition, emissions from two hairdryers primarily contained silver nanoparticles in the ultrafine range (<100 nm). The ultrafine particle emission rates for the hairdryers that did not contain silver were measured and found to be on the same order of magnitude as ultrafine particle emissions by gas stoves and electric burners. Based on their size, these particles can either remain in the lung or enter into the bloodstream after inhalation and potentially cause long term health effects.

**Keywords:** Air pollution · Particulate matter · Human health · Nanoparticles · Silver

## Synopsis

Hairdryers emit ultrafine particles which can be harmful to human health. This paper characterizes the emissions of several hairdryers.

30 **Introduction**

31 In 1977 the U. S. Clean Air Act was amended to reflect the growing concern of
32 the influence of inhalable particulate matter on human health. Since then, particulate air
33 pollution has been classified into three main categories: coarse particles (< 10 μm, $PM_{10}$),
34 fine particles (< 2.5 μm, $PM_{2.5}$), and ultrafine particles (< 100 nm, $PM_{0.1}$). These
35 divisions are made to reflect the potential health impact of each size regime. Historically,
36 the impact of outdoor air pollution on human health was the emphasis of research studies.
37 For example, the Harvard Six Cities study outlined a direct correlation between fine
38 particulate matter and mortality.[1] Those results have been confirmed and expounded upon
39 revealing that $PM_{2.5}$ is capable of entering deep into the lungs and becomes embedded in
40 the alveolar sacs, increasing the burden of cardiopulmonary disease, diabetes, and
41 preterm birth.[2-5] The mechanisms of toxicity include oxidative stress, mutagenicity and
42 genotoxicity, and inflammatory response.[5] In addition to the negative health effects
43 caused by particulate matter, it is currently estimated that the aggregate social cost, the
44 cost associated with treating diseases, of particulate matter in the United States is $330
45 billion per year.[6] In more recent years, ultrafine particulate matter has been identified as a
46 cause for concern. Studies in rats revealed that when inhaled, these particles can enter
47 into the bloodstream in as little as fifteen minutes.[7] Upon entering the bloodstream,
48 particles can interact with the body on a cellular level. This cellular interaction is
49 dependent on the composition, size, and surface properties of the nanoparticle, and the
50 dependence of toxicity on composition is complex. Ultrafine particles have been
51 associated with respiratory diseases, cardiovascular diseases, diabetes, cancer, and

negative effects on the brain and central nervous system.[8, 9] While the field of nanotoxicology is fairly new, the effect of metal nanoparticles, such as, gold, silver, titanium dioxide, and iron oxide have been investigated.[10] Once absorbed into the bloodstream, metal nanoparticles have been shown to cause oxidative stress and mitochondrial damage.[11] Even if these particles do not enter the bloodstream, they can cause irritation of the lung by depleting antioxidants in the lung lining fluid and initiating oxidative stress.[12] As concern over the impact of particulate matter continues to rise, compositional information will be key to understanding the full health effects of ultrafine particles.

While much focus has been placed on outdoor air pollution, Americans spend approximately 87% of their time indoors, and daily activities like cooking and cleaning release particulate matter into the air.[13] Additionally, particulate matter from outside can transfer indoors where it can dwell for long periods of time. High particle number concentrations and large particle surface areas result in an increased number of particles being absorbed into the bloodstream, or otherwise deposited onto tissues.[14, 15] Many household items and activities, such as cigarette smoking, candle burning gas stove operation and heated surfaces, serve as sources of ultrafine particles.[2, 15-20] Indoor sources of particulate matter generally generate much less particulate matter than outdoor/industrial sources, but because these particles are confined in small room volumes they can quickly exceed the EPA's National Ambient Air Quality Standards (NAAQS).[20, 21] Exposure to indoor pollutants such as open burning fires can be greater and cause more cognitive impairment that outdoor exposure to pollutants such as commuting on heavily-trafficked roads (Maher et al. 2021). Ultrafine particles have high

75 mobility and quickly coagulate to form larger particles. The risk associated with these
76 particles is therefore dependent on the rates of emission, aggregation, and deposition.[15, 20,
77 22] These rates determine the number and size of the particles as a function of distance
78 from the source. A recent campaign (HOMEChem) has used a test home to investigate
79 the gas, particle and surface chemistry in the indoor environment.[23-27] These studies
80 focused on the impacts of ventilation and addressed influence of organic aerosol particles
81 and gas phase pollutants.

82 Due to the ability of nanoparticles to enter into the bloodstream, size distribution
83 information alone is not enough to fully understand their impact on human health. The
84 emerging field of nanotoxicology attempts to elucidate the health impacts of
85 nanoparticles based on their composition and size.[10, 28, 29] Understanding the full effects
86 of indoor air pollution lies in the composition of the ultrafine particulate matter. Recent
87 literature has focused on household sources of silver nanoparticles. Silver nanoparticles
88 are well known antimicrobial agents and many products seek to benefit from those
89 properties.[30, 31] Quadros and Marr identified various household antimicrobial sprays as
90 containing silver nanoparticles.[32] Further work has been done by Taylor et al. on types of
91 hairdryers that are marketed for containing antimicrobial silver nanoparticles, as potential
92 sources of silver nanoparticles.[33] The close proximity of hairdryers to human airways
93 during operation could allow an increase in the localized concentration of silver
94 nanoparticles. As an antimicrobial agent, silver nanoparticles induce oxidative stress
95 within the body. There are no guidelines established by the EPA to regulate the inhalation
96 of silver nanoparticles, however OSHA has a set exposure limit of 0.01 mg $m^{-3}$ for

97 metallic silver and recent literature has highlighted the cytotoxic effects of silver
98 nanoparticles.[15, 29, 34]

99 In this paper, the ultrafine particles emitted from hairdryers are characterized,
100 with a focus on silver nanoparticles due to their specific health effects. Hairdryers were
101 selected based on user-specified popularity, and operated under controlled conditions so
102 that the particles generated could be studied. The emission rate of ultrafine particles were
103 determined and an elemental characterization of these particles was performed using
104 TEM and EDS.

## 105 Materials and Methods

### 106 *Hairdryers*

107 Six hairdryers were selected for investigation based on the "most popular" listing
108 of hairdryers on Amazon.com at the time of purchase. These included five new and
109 unused hairdryers, and one heavily used hairdryer. The following unused hairdryers were
110 tested: Revlon 1875-watt ceramic, ion hairdryer (Model RV484), Remington Pro (Model
111 D3190), Ovonni (Model BST-808I), Ionic Turbo (Model HTDR5577SN2), and ConAir
112 1875 Watt (Model 247). The heavily used, approximately five-year-old hairdryer, was a
113 Revlon 1875-watt hairdryer (Model RVDR5034). The older hairdryer was used to see if a
114 different distribution of particles was observed after long term use.

115 ***Particle Generation and Collection***

116 A 127.5 L Plexiglass chamber was built to house the hairdryers during operation
117 to eliminate the influence of ambient aerosol particles (Figure 1).[35] In contrast, a previous
118 study with hairdryers was performed in open air without a chamber, where the
119 background levels of aerosol particles are high.[33] Our chamber was purged with
120 prepurified nitrogen gas at a flow rate of 1.5 L $min^{-1}$ for approximately 30 min.
121 Afterward, a condensation particle counter (TSI 3775, Shoreview, MN) was used to
122 verify that the concentration of particles within the chamber had reached a minimum.
123 Each hairdryer was then operated on the lowest setting for 1 min while maintaining a
124 constant 1.5 L $min^{-1}$ flow of prepurified nitrogen. Using a cascade impactor (PIXE
125 International Corp., Tallahassee, FL, USA) particles were collected onto 200 mesh
126 copper TEM grids coated with a continuous carbon coating (Electron Microscopy
127 Science, Hatfield, PA). The cutoff diameter of the impactor stage used is 250 nm. It was
128 assumed that the fan within the hairdryer was sufficient to maintain a well-mixed
129 chamber and thus a mixing fan was not used.

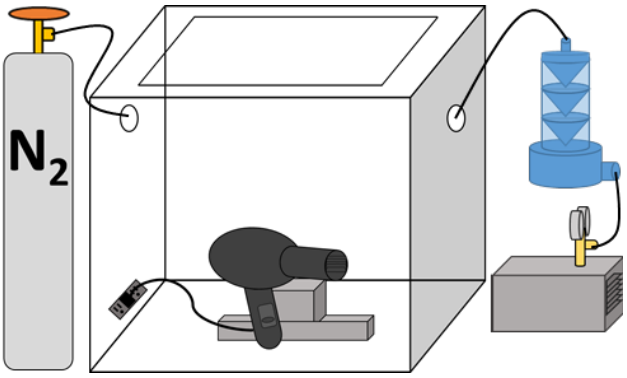


130

131 **Figure 1:** Schematic figure of hairdryer experimental set-up showing nitrogen input,
132 impactor, and pump.

133 ***Characterization of Chamber and Emission Calculations***

134 To determine the emission rates of the hairdryers, the 127.5 L Plexiglass chamber
135 was characterized. First, the air exchange rate (AER) was determined by first filling the
136 chamber with 2500 ppmv $CO_2$ and then flowing clean air into the chamber at a rate of 1.5
137 L $min^{-1}$. A vacuum pump was used to match the flowrate entering the chamber by pulling
138 on the chamber at a rate of 1.5 L $min^{-1}$. The concentration of $CO_2$ was monitored with a
139 HOBOware Onset data logger (U12-013 logger, Telaire 7001 $CO_2$ sensor). The rate of
140 decay for the $CO_2$ was determined and is the AER. Next the particle deposition rate
141 within the chamber was determined. This was done by filling with chamber with
142 aerosolized 200 nm polystyrene spheres latex beads (PSLs) using an atomizer (TSI 3075)
143 and an air flow rate of 1.5 L $min^{-1}$. The chamber was continually filled with these
144 aerosolized PSLs until the concentration of particles was stable. The particle
145 concentration was monitored and recorded using a condensation particle counter (CPC,
146 TSI 3775). Once the concentration stabilized, the generation of aerosol was halted but a
147 clean purge flow at a rate of 1.5 L $min^{-1}$ was maintained. The rate of decay of the
148 particles while a purge flow was maintained was then determined. Representative time
149 traces from the air exchange and deposition rate measurements are shown in Fig. S1. To
150 determine the particle deposition rate, the air exchange rate was subtracted from the
151 particle decay rate with a purge flow. Each hairdryer was operated at its lowest setting in
152 the chamber while maintaining a purge flow of 1.5 L $min^{-1}$ for 30 min, which exceeded
153 the time required for the particle concentration to reach a maximum and steady value.
154 Note that the hairdryers do warm up the chamber during operation, which could result in

155 some particles reemitting from the walls of the chamber. After 30 min the hairdryer was
156 turned off while the purge flow continued for another 30 min. Particle emission rates (S)
157 were calculated by

158 $$S = \frac{V(a+k)C_{peak}}{1-e^{(a+k)t}} \quad (1)$$

159 where $V$ is the volume of the chamber, $C_{peak}$ is maximum concentration of the particles
160 before they began to decay, $a$ is the air exchange rate, $k$ is the particle deposition rate, and
161 $t$ is the time at $C_{peak}$.[32] These emission rates were determined for the particles in the
162 ultrafine range, therefore particles greater than 100 nm in diameter were not included in
163 the particle counts. This was done by acquiring a SMPS profile and adding together the
164 particle counts for particles less than 100 nm. Representative emission rate time traces
165 and SMPS size distributions are shown in Figs. S2 and S3. Note that the SMPS
166 characterizes particles by their electrostatic mobility diameter rather than their geometric
167 size. The theory for which particles are transmitted by the SMPS in a certain size bin
168 assumes that the particles are spherical. The transmission of particles is independent of
169 their composition.

170 ***Particle Characterization***

171 A Tecnai G20 20 XTWIN transmission electron microscope (FEI, Hillsboro, OR)
172 with an accelerating voltage of 200 keV was used to acquire images of particles
173 generated by the hairdryer. This electron microscope is equipped with an EDAX Apollo
174 XLT 30mm$^2$ silicon drift detector energy dispersive spectrometer (EDS) with a super
175 ultra-thin window. This EDS detector was used to obtain point EDS spectra to quickly

176 characterize particle composition. EDS maps were obtained with a FEI Talos F200X
177 scanning/transmission electron microscope (FEI, Hillsboro, OR) with an accelerating
178 voltage of 200 keV using the Super-X EDS windowless, quad silicone drift detector
179 system at a current of -0.15 nA and a solid angle of 0.9 srad. ImageJ software (NIH) was
180 used to determine the area equivalent diameters of each particle analyzed from the digital
181 micrographs.

182 ***Characterization of Composition of Hairdryer Components***

183 To determine the source of the silver nanoparticles coming from the hairdryers,
184 their components were studied. The Revlon 1875-watt hairdryer (Model RVDR5034)
185 was disassembled and its components isolated for analysis with inductively coupled
186 plasma emission spectrometry (ICP-AES). Small samples were obtained from each
187 unique component. Each sample was digested in acid and analyzed via a Perkin-Elmer
188 Optica 5300 UV ICP-AES for silver concentration. Additionally, a duplicate hairdryer of
189 the same model that had never been operated was analyzed in the same manner.

190 **Results and Discussion**

191 The air exchange rate for the 127.5 L Plexiglass chamber was found to be 0.754 ±
192 0.060 $h^{-1}$ and the particle deposition rate was found to be 0.234 ± 0.190 $h^{-1}$. High standard
193 deviations in particle deposition rates are common and not unexpected in this case, in part
194 due to the fact that particle deposition rates depend on particle size.[36-40] The emission rate

195 of ultrafine particles was determined for four of the hairdryers. The emission rate for the
196 Remington Pro (Model D3190) was found to be $2.60 \times 10^{12} \pm 1.47 \times 10^{12}$ $h^{-1}$, for the
197 Ovonni (Model BST-808I) it was $1.64 \times 10^{12} \pm 0.07 \times 10^{12}$ $h^{-1}$, for the ConAir 1875 Watt
198 (Model 247) it was $4.25 \times 10^{12} \pm 0.36 \times 10^{12}$ $h^{-1}$, and for the Ionic Turbo (Model
199 HTDR5577SN2) it was $1.27 \times 10^{12}$ $h^{-1} \pm 0.42 \times 10^{12}$ $h^{-1}$. Note that the uncertainty shown
200 represents the variation over the measurement period. Due to the destructive nature of
201 the ICP-AES experiments conducted, the emission rates for the Revlon hairdryers were
202 not determined, however since the other four hairdryers produced ultrafine particles on
203 the same order of magnitude, we expect these hairdryers to be in the same range. The
204 concentration of ultrafine particles generated by the hairdryers were on the same order of
205 magnitude as ultrafine particle emissions by gas stoves and electric burners, and an order
206 of magnitude higher than ultrafine particle emissions by candles.[41] Note that the cited
207 measurements were taken in a full scale, single-story test house with a floor area of 140
208 $m^2$. Measurement of the particles generated by the gas and electric stoves were taken in
209 the master bedroom, giving an indication of the quantity of particles that travel
210 throughout the house. The measurement of candle emissions was taken in the same room
211 as the source.[41] These measurement conditions and results suggest that hairdryers
212 produce a lower concentration of particles than gas and electric stoves and a higher
213 concentration than candles.

214 **Table 1**: Hairdryer emissions rates determined by the chamber studies and compositions
215 of particles determined by EDS for the six hairdryers in this study.

| Hairdryer | Emission Rate ($x10^{12}$ $h^{-1}$) | Size Distribution Comments | Composition |
|---|---|---|---|
| **Remington Pro (Model D3190)** | $2.60 \pm 1.47$ | N/A | Iron, Carbon, Copper |
| **Ovonni** | $1.64 \pm 0.07$ | N/A | Iron, Carbon, Copper |

| | | | |
|---|---|---|---|
| **(Model BST-808I)** | | | |
| **ConAir 1875 Watt (Model 247)** | $4.25 \pm 0.36$ | N/A | Iron, Carbon, Copper |
| **Ionic Turbo (Model HTDR5577SN2)** | $1.27 \pm 0.42$ | N/A | Iron, Carbon, Copper |
| **Revlon 1875 Watt (Model RVDR5034)** | N/A | Bimodal | Silver, Nickel, Iron, Carbon, Copper |
| **Revlon 1875 Watt ceramic, ion hairdryer (Model RV 484)** | N/A | Bimodal | Silver, Nickel, Iron, Carbon, Copper |

Of the six hairdryers investigated all emitted particles in the ultrafine range. Emission rates, particle compositions, and distribution types for these hairdryers are tabulated in Table 1. EDS spectra were acquired with the EDAX Apollo XLT system and the spectra were used to characterize the composition of particles from each hairdryer. Each of the hairdryers emitted particles composed of iron and likely particles composed of copper and carbon. Due to the presence of copper and carbon in the grid however, the determination of these elements in the sample may be unreliable. It should be noted that the relative intensity of the EDS signals does strongly suggest that some particles were composed of carbon and/or copper because they are higher than the background level. Copper and iron are redox active and are known to cause oxidative stress in models for lung epithelial tissue.[42-44] We have focused below on the silver nanoparticles found in two hairdryers due to current interest in their fate in the environment as a result of their growing use in consumer products as antimicrobial agents. Most notably, two of the hairdryers, the Revlon 1875-watt ceramic, ion hairdryer (Model RV484) and the Revlon 1875-watt hairdryer (Model RVDR5034) primarily emitted silver nanoparticles (Figure 2). As a result, these hairdryers were analyzed in more detail. Of the 283 particles analyzed, 81% of particles contained silver. This result is in contrast to the work of

Taylor et al. who used scanning electron microscopy paired with EDS. This technique was limited to particles greater than 56 nm and as a result, no silver was detected during their study.[33] It should be noted that the hairdryers used in this study were not marketed as containing silver nanoparticles, while the study performed by Taylor et al. included hairdryers marketed in this manner[33]. Note also that because our experiments were performed under $N_2$ gas rather than air, the particles may not be as highly oxidized as they would be in an environmental sample.

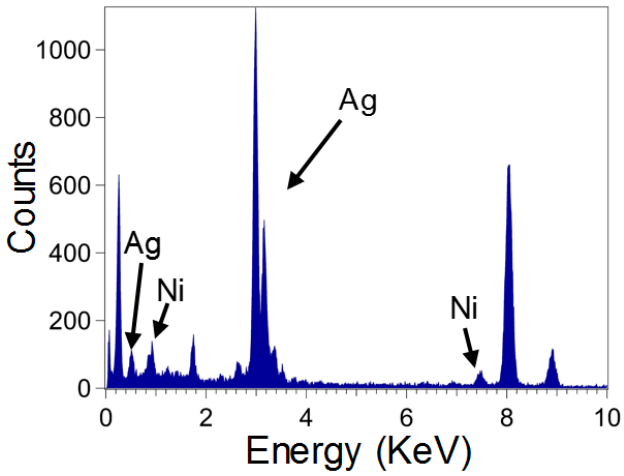


**Figure 2:** A representative point EDS spectrum of a particle emitted by the Revlon 1875-watt ceramic, ion hairdryer (Model RV484).

The other four hairdryers had a primary emission of carbon containing nanoparticles, which were likely organic compounds reemitted from the heating elements within the hairdryers or otherwise combustion products from the material burning on the high temperature heating elements. We note that a representative TEM image of the hairdryer emissions of the Revlon Model RV484 is shown in Figure 3a. 92.3 % of

imaged particles from this hairdryer were nanoparticles in the ultrafine range. The particles are highly crystalline, exhibiting lattice fringes. The high contrast in the images indicates that they are composed of atoms with high Z-numbers. The smallest particles that were observed in this analysis were approximately 1.5 nm in area equivalent diameter, and the largest particles were about 250 nm. Figure 3b shows one such large aggregate surrounded by many much smaller particles that are believed to have separated from the aggregate.[45] These large particles that are outside the ultrafine range were observed to be large aggregates. We focused on the particles in the ultrafine range due to their ability to potentially cross from the lungs to the bloodstream. Larger particles and very small particles (< 10 nm) are more easily filtered and deposit in the upper airway and thus pose less of a health risk. The aggregates seen in Fig. 3b are interesting in part because these larger particles may travel deeper into the respiratory system and could subsequently break apart and cross into the bloodstream. Of the total population of observed particles, sizes were as small as 4 nm. Unlike with the previously unused Revlon Model RV484, silver nanoparticles greater than 60 nm were observed in the emissions from the used Revlon Model RVDR5034. This result is likely due to aggregates of particles.

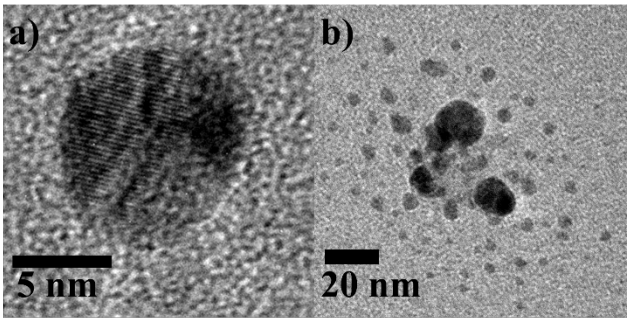

**Figure 3:** a) Representative TEM image of a single silver nanoparticle. b) Representative TEM image of a broken silver nanoparticle aggregate.

To gain a more comprehensive understanding of particles containing silver and nickel, and to subtract out background signals from the detector and grids, representative particles from the Revlon hairdryers were characterized with EDS mapping. The mapping software (ESpirit) allows for a quantitative elimination of background signal and the mapping itself allows for spatial resolution of particle composition. EDS mapping revealed that particles from the used hairdryer were primarily composed of silver with some nickel on the edges of the particles. It should be noted that while EDS provides elemental information, it does not indicate what form the element is in, and therefore the silver and nickel could be in their elemental forms or exist as oxides. A representative map of one of these particles is shown in Figure 4.

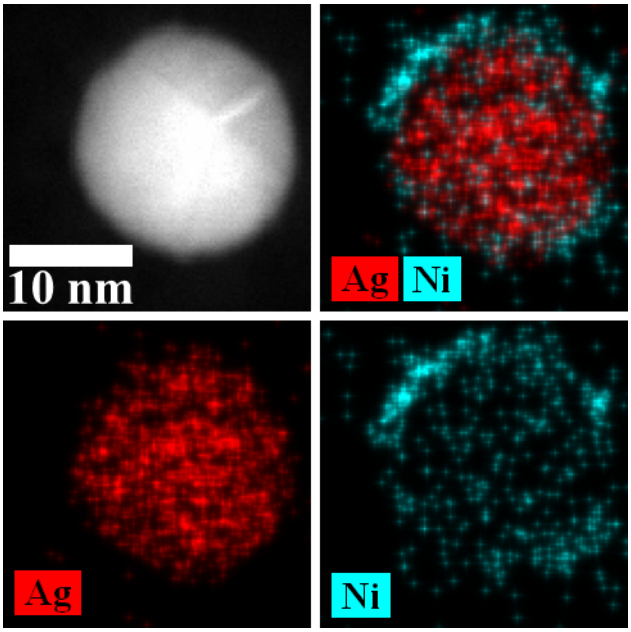


**Figure 4:** EDS map of a representative silver nanoparticle emitted by the used Revlon 1875-watt ceramic, ion hairdryer (Model RV484).

284 Using the data from the point EDS spectra, size resolved histograms were
285 generated for the silver nanoparticles. The particles had a bimodal distribution centered
286 on the 5 nm and 25 nm bins and 0 particles out of the 229 counted were > 100 nm (Figure
287 5a). The 5 nm bin is exceptionally high compared to the larger size bins. The large
288 population in this bin is hypothesized to be due to loosely aggregated particles breaking
289 free from one another upon impaction with the TEM grid (Figure 3b). This behavior has
290 previously been observed when quartz is impacted onto $SiO_x$/Si substrates for scanning
291 electron microscopy.[46] This hypothesis is further supported by the morphology of
292 particles that were not aggregated, as shown in Figure 6. In this EDS map, many small
293 (<5 nm) particles appear to be loosely aggregated to a large nickel particle. This is not to
294 say that the <5 nm particles are created by the aggregates, but that they have been there
295 all along, and they are easier to locate and count during a TEM session due to their
296 proximity to a larger more visible particle. Particles <5 nm shown in the histogram
297 maybe, at least in part, due to these aggregates.

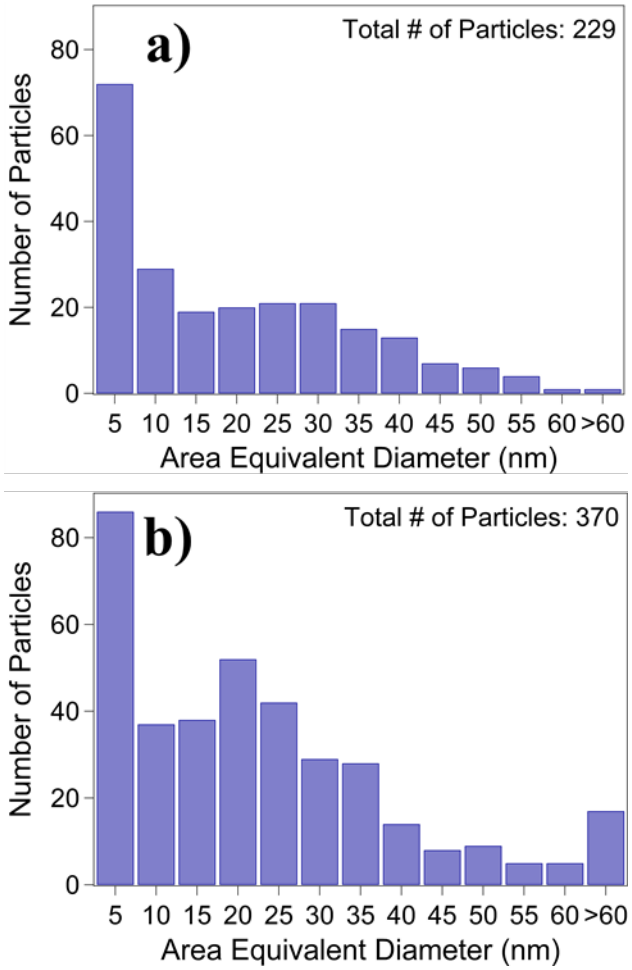


**Figure 5:** a) Histogram of particle sizes for silver-containing particles emitted by the Revlon Model RVDR5034 (new) hairdryer (median diameter = 13.8 nm). B) Histogram of particle sizes for silver-containing particles emitted by the Revlon Model RV484 (used) hairdryer (median diameter = 16.9 nm).

Similar results were obtained from the used hairdryer with the bimodal distribution again centered on the 5 nm and 25 nm size bins (Figure 5b). In contrast to the new hairdryer, this sample contained a significant number of particles greater than 60 nm in diameter. In this case, 5 particles out of 370 counted had diameters > 100 nm. A representative image of one of these large aggregates is shown in Figure 6a. Again, point EDS revealed that the particles from the used hairdryer were primarily composed of silver. Interestingly, particles that were greater than 60 nm were found to be composed of

Ni aggregated with small silver particles, as indicated by EDS mapping (Figure 6b). This kind of aggregation was not observed in the hair dryers that did not contain silver; however, some of the particles primarily composed of iron appeared to be coated in a carbon containing compound.

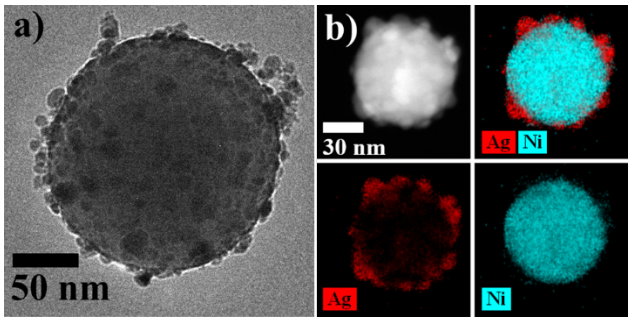


**Figure 6:** a) TEM image of a large aggregate emitted by the Revlon Model RVDR5034 hairdryer. b) EDS maps showing that the large aggregates emitted by the Revlon Model RVDR5034 hairdryer are nickel nanoparticles with smaller silver nanoparticles aggregated to them.

To determine the origin of the silver nanoparticles generated by the Revlon Model RVDR5034 hairdryer, it was carefully disassembled and each of the components were separated. All samples contained some silver, as expected due to the extended operation of the hairdryer. When the hairdryer is powered on and silver particles are generated, it is very likely that they are able to travel throughout the hairdryer and accumulate on all components.

The two components with the highest weight percent silver were the solder connecting the power cord to the switches in the handle of the hairdryer with 0.029 ± 0.001 wt% silver, and the metallic, foil-like cover surrounding the heating coil in the head of the hairdryer with 0.038 ± 0.002 wt% silver, marking these two components as the possible primary sources of silver nanoparticles. The heating coil cover has the largest surface area of all components and covers most of the interior of the hairdryer head,

raising the possibility that the majority of silver particles settle on this component during operation of the hairdryer as opposed to originating here. A second Revlon 1875-watt hairdryer (Model RVDR5034) was purchased, and immediately, without any operation of the hairdryer after distribution, samples of the same components were isolated and submitted for ICP-AES analysis. Unlike the first analysis, neither the metallic cover nor the solder contained the highest concentrations of silver. This validates the theory that the cover is accumulating silver during operation. Even without operating the device there was evidence of silver, ranging from 0.003 wt% to 0.020 wt%, in many different components indicating that there may not be any one major source of silver within the hairdryer, but rather multiple smaller sources. After continual operation, much of the silver collects onto the foil-like cover. The size scale of the particles emitted by the hairdryers is alarming as the particles in this range are easily inhaled and can enter the bloodstream. While we cannot directly compare the two hairdryers, it is to be noted that despite heavy usage over a long period, the used hairdryer still produced silver nanoparticles. This result indicates that long term exposure to silver is possible. Note also that the components found to contain silver are very common, but the emission of silver nanoparticles was only found for these two hairdryers.

The emissions from six different hairdryers were analyzed. All of the hairdryers were found to emit particles in the ultrafine range. Particles in the ultrafine range are known to cause adverse health effects such as cardiovascular and pulmonary diseases.[3] The hairdryer ultrafine emission rates were found to be less than the ultrafine emissions of gas and electric stoves and more than measurements of ultrafine emissions from candles. Primarily, the particles measured with TEM were observed to be spherical.

354 Some research suggests that knowing the shape of these nanoparticles may be beneficial
355 for the future of toxicological studies of indoor air pollution since some shapes may more
356 easily pass into cells than others.[47] While in general, the hairdryers emitted particles
357 composed of iron, copper, and carbon; the two Revlon hairdryers were shown to generate
358 silver nanoparticles in the ultrafine particle range. Ultrafine silver particles have been
359 shown to pose additional negative health effects in addition to those caused by
360 uncategorized ultrafine particles.[31] Specifically, silver nanoparticles can cause oxidative
361 stress within cells which can lead to cellular death.[15] Larger silver containing particles
362 were found to be the result of aggregation of ultrafine particles. The Revlon 1875-watt
363 hairdryer (Model RVDR5034) used in the study and a duplicate hairdryer were both
364 disassembled and the components were tested for silver with ICP-AES. While no one
365 component was the main source of silver, many components were found to contain silver.
366 Due to their antimicrobial properties, silver nanoparticles can be harmful if they enter
367 into the bloodstream and the particles observed in this study were small enough to pass
368 through the blood-air barrier if inhaled. Even if such particles remain in the lungs they
369 can cause irritation of the lung lining, which can lead to the onset of disease. Indoor air
370 pollution sources are potentially harmful when operated in locations with poor
371 ventilation. Without a removal method, ultrafine particulate matter produced by indoor
372 sources can reach high concentrations. Sources, such as hairdryers, are often operated
373 close to human airways and thus even when ventilation is available the proximity to
374 pollution source may result in exposure to high concentrations of particles.
375
376 **Supporting Information**

Representative time traces for air exchange, particle deposition, and emission rate measurements. Size distributions for particles emitted from hairdryers.

## Author Information

Corresponding Author

*To whom all correspondence should be addressed: maf43@psu.edu, 814-867-4267

## Acknowledgments

The authors gratefully acknowledge support from the NSF CAREER program (CHE-1351383) and a seed grant from Penn State's Institute of Energy and the Environment. J. N. D. acknowledges funding from the NSF GRFP (NSF 1255832). We acknowledge the Materials Characterization Lab run by the Penn State Materials Research Institute for use of the FEI Talos and FEI Tecnai electron microscopes. We thank J. Gray and K. Wang from the Penn State Materials Research Institute for their expert feedback and assistance. We thank L. Liermann for her assistance with the ICP-AES. We are grateful to D. Rim for helpful discussions.

## References


1. Dockery, D. W.; Pope, C. A.; Xu, X.; Spengler, J. D.; Ware, J. H.; Fay, M. E.; Ferris, B. G.; Speizer, F. E., An Association between Air Pollution and Mortality in Six U.S. Cities. *New England Journal of Medicine* **1993,** *329*, (24), 1753-1759.
2. Pope III, C. A.; Thun, M. J.; Namboodiri, M. M.; Dockery, D. W.; Evans, J. S.; Speizer, F. E.; Clark W. Heath, J., Particulate Air Pollution as a Predictor of Mortality in a Prospective Study of U.S. Adults. *American Journal of Respiratory and Critical Care Medicine* **1995,** *151*, (3), 669-674.
3. Pope III, C. A.; Burnett, R. T.; Thun, M. J.; Calle, E. E.; Krewski, D.; Ito, K.; Thurston, G. D., Lung Cancer, Cardiopulmonary Mortality, and Long-term Exposure to Fine Particulate Air Pollution. *JAMA* **2002,** *287*, (9), 1132-1141.
4. Miller, K. A.; Siscovick, D. S.; Sheppard, L.; Shepherd, K.; Sullivan, J. H.; Anderson, G. L.; Kaufman, J. D., Long-Term Exposure to Air Pollution and Incidence of Cardiovascular Events in Women. *New England Journal of Medicine* **2007,** *356*, (5), 447-458.
5. Feng, S.; Gao, D.; Liao, F.; Zhou, F.; Wang, X., The health effects of ambient PM2.5 and potential mechansims,. *Ecotoxicology and Environmental Safety* **2016,** *128*, 67-74.
6. Heo, J.; Adams, P. J.; Gao, H. O., Public Health Costs of Primary PM2.5 and Inorganic PM2.5 Precursor Emissions in the United States. *Environmental Science & Technology* **2016,** *50*, (11), 6061-6070.
7. Oberdörster, G.; Celein, R. M.; Ferin, J.; Weiss, B., Association of Particulate Air Pollution and Acute Mortality: Involvement of Ultrafine Particles? *Inhalation Toxicology* **1995,** *7*, (1), 111-124.
8. Ohlwein, S.; Kappeler, R.; Joss, M. K.; Künzli, N.; Hoffmann, B., Health effects of ultrafine particles: a systematic literature review update if epidemiological evidence. *International Journal of Public Health* **2019**, 64, 547-559.
9. Schraufnagel, D., The health effects of ultrafine particles. *Experimental & Molecular Medicine* **2020**, 52, 311-317.
10. Nel, A. E.; Mädler, L.; Velegol, D.; Xia, T.; Hoek, E. M. V.; Somasundaran, P.; Klaessig, F.; Castranova, V.; Thompson, M., Understanding biophysicochemical interactions at the nano–bio interface. *Nature Materials* **2009,** *8*, (7), 543-557.
11. Oberdörster, G.; Oberdörster, E.; Oberdörster, J., An emerging discipline evolving from studies of ultrafine particles supplemental web sections. *Environ. Health Perspect* **2005,** *113*, (7), 823-839.
12. W. Yang, S. T. Omaye, Air Pollutants, Oxidative Stress, and Human Health, Mutation Research, 2009, 674, 45-54.
13. Klepeis, N. E.; Nelson, W. C.; Ott, W. R.; Robinson, J. P.; Tsang, A. M.; Switzer, P.; Behar, J. V.; Hern, S. C.; Engelmann, W. H., The National Human Activity Pattern Survey (NHAPS): a resource for assessing exposure to environmental pollutants. *Journal of Exposure Science & Environmental Epidemiology* **2001,** *11*, (3), 231-252.
14. Nel, A.; Xia, T.; Mädler, L.; Li, N., Toxic Potential of Materials at the Nanolevel. *Science* **2006,** *311*, (5761), 622-627.
15. Verma, A.; Stellacci, F., Effect of Surface Properties on Nanoparticle–Cell Interactions. *Small* **2010,** *6*, (1), 12-21.
16. Hussein, T.; Glytsos, T.; Ondráček, J.; Dohányosová, P.; Ždímal, V.; Hämeri, K.; Lazaridis, M.; Smolík, J.; Kulmala, M., Particle size characterization and emission rates during indoor activities in a house. *Atmospheric Environment* **2006,** *40*, (23), 4285-4307.

17. Géhin, E.; Ramalho, O.; Kirchner, S., Size distribution and emission rate measurement of fine and ultrafine particle from indoor human activities. *Atmospheric Environment* **2008,** *42*, (35), 8341-8352.
18. Pagels, J.; Wierzbicka, A.; Nilsson, E.; Isaxon, C.; Dahl, A.; Gudmundsson, A.; Swietlicki, E.; Bohgard, M., Chemical composition and mass emission factors of candle smoke particles. *Journal of Aerosol Science* **2009,** *40*, (3), 193-208.
19. Wallace, L.; Wang, F.; Howard-Reed, C.; Persily, A., Contribution of Gas and Electric Stoves to Residential Ultrafine Particle Concentrations between 2 and 64 nm: Size Distributions and Emission and Coagulation Rates. *Environmental Science & Technology* **2008,** *42*, (23), 8641-8647.
20. Rim, D.; Choi, J.-I.; Wallace, L. A., Size-Resolved Source Emission Rates of Indoor Ultrafine Particles Considering Coagulation. *Environmental Science & Technology* **2016,** *50*, (18), 10031-10038.
21. U.S. EPA National Ambient Air Quality Standards for Particulate Matter. www.epa.gov/criteria-air-pollutants/naaqs-table (November 27, 2020),
22. Nazaroff, W. W., Indoor particle dynamics. *Indoor Air* **2004,** *14*, (Supplement 7), 175-183.
23. Ampollini, L.; Katz, E. F.; Bourne, S.; Tian, Y.; Novoselac, A.; Goldstein, A. H.; Lucic, G.; Waring, M. S.; DeCarlo, P. F., Observations and Contributions of Real-Time Indoor Ammonia Concentrations during HOMEChem. *Environmental Science & Technology* **2019,** *53*, (15), 8591-8598.
24. Farmer, D. K.; Vance, M. E.; Abbatt, J. P. D.; Abeleira, A.; Alves, M. R.; Arata, C.; Boedicker, E.; Bourne, S.; Cardoso-Saldaña, F.; Corsi, R.; DeCarlo, P. F.; Goldstein, A. H.; Grassian, V. H.; Hildebrandt Ruiz, L.; Jimenez, J. L.; Kahan, T. F.; Katz, E. F.; Mattila, J. M.; Nazaroff, W. W.; Novoselac, A.; O'Brien, R. E.; Or, V. W.; Patel, S.; Sankhyan, S.; Stevens, P. S.; Tian, Y.; Wade, M.; Wang, C.; Zhou, S.; Zhou, Y., Overview of HOMEChem: House Observations of Microbial and Environmental Chemistry. *Environmental Science: Processes & Impacts* **2019,** *21*, (8), 1280-1300.
25. Katz, E.; Boedicker, E.; Brown, W.; Day, D. A.; Jimenez, J. L.; Farmer, D.; Vance, M.; Patel, S.; DeCarlo, P. F., Insights on Indoor Aerosol Emissions during the HOMEChem Campaign and Potential Implications for Source Apportionment of Ambient Organic Aerosols. In 2019; Vol. 2019, pp U14C-11.
26. Patel, S.; Sankhyan, S.; Boedicker, E. K.; DeCarlo, P. F.; Farmer, D. K.; Goldstein, A. H.; Katz, E. F.; Nazaroff, W. W.; Tian, Y.; Vanhanen, J.; Vance, M. E., Indoor Particulate Matter during HOMEChem: Concentrations, Size Distributions, and Exposures. *Environmental Science & Technology* **2020,** *54*, (12), 7107-7116.
27. Tian, Y.; Arata, C.; Boedicker, E.; Lunderberg, D. M.; Patel, S.; Sankhyan, S.; Kristensen, K.; Misztal, P. K.; Farmer, D. K.; Vance, M., Indoor emissions of total and fluorescent supermicron particles during HOMEChem. *Indoor Air* **2021**, *31*, 88-98.
28. Blaser, S. A.; Scheringer, M.; MacLeod, M.; Hungerbühler, K., Estimation of cumulative aquatic exposure and risk due to silver: Contribution of nano-functionalized plastics and textiles. *Science of The Total Environment* **2008,** *390*, (2), 396-409.
29. Rai, M.; Yadav, A.; Gade, A., Silver nanoparticles as a new generation of antimicrobials. *Biotechnology Advances* **2009,** *27*, (1), 76-83.
30. Maillard, J.-Y.; Hartemann, P., Silver as an antimicrobial: facts and gaps in knowledge. *Critical Reviews in Microbiology* **2013,** *39*, (4), 373-383.
31. Yang, X.; Gondikas, A. P.; Marinakos, S. M.; Auffan, M.; Liu, J.; Hsu-Kim, H.; Meyer, J. N., Mechanism of Silver Nanoparticle Toxicity Is Dependent on Dissolved Silver and Surface

Coating in Caenorhabditis elegans. *Environmental Science & Technology* **2012,** *46*, (2), 1119-1127.
32. Quadros, M. E.; Marr, L. C., Silver Nanoparticles and Total Aerosols Emitted by Nanotechnology-Related Consumer Spray Products. *Environmental Science & Technology* **2011,** *45*, (24), 10713-10719.
33. Taylor, A. A.; Khan, M. Y.; Helbley, J.; Walker, S. L., Safety evaluation of hair-dryers marketed as emitting nano silver particles. *Safety Science* **2017,** *93*, 121-126.
34. U.S. Dept. of Labor. OSHA Permissible Exposure Limits / OSHA Annotated Table Z-1. www.osha.gov/dsg/annotated-pels/tablez-1.html (November 28, 2019),
35. Afshari, A.; Matson, U.; Ekberg, L. E., Characterization of indoor sources of fine and ultrafine particles: a study conducted in a full-scale chamber. *Indoor Air* **2005,** *15*, (2), 141-150.
36. L. Wallace, S.-G. Jeong, D. Rim, Dynamic Behavior of Indoor Ultrafine Particles (2.3 – 64 nm) due to burning candles in a residence, Indoor Air, 2019, 29, 1018-1027.
37. W. W. Nazaroff, Indoor Particle Dynamics, Indoor Air, 2004, 14, 175-183.
38. Donghyun Rim , Michal Green , Lance Wallace , Andrew Persily & Jung-Il Choi (2012) Evolution of Ultrafine Particle Size Distributions Following Indoor Episodic Releases: Relative Importance of Coagulation, Deposition and Ventilation, Aerosol Science and Technology, 46:5, 494-503.
39. A. C. K. Lai, Particle Deposition Indoors: A Review, Indoor Air, 2002, 12, 211-214.
40. T. Hussein, L. Kubincová, L. Džumbová, A. Hruška, P. Dohányosová, J. Hemerka, J. Smolík, Deposition of Aerosol Particles on Rough Surfaces Inside a Test Chamber, Building and Environment, 2009, 44, 2056-2063.
41. Rim, D.; Green, M.; Wallace, L.; Persily, A.; Choi, J.-I., Evolution of Ultrafine Particle Size Distributions Following Indoor Episodic Releases: Relative Importance of Coagulation, Deposition and Ventilation. *Aerosol Science and Technology* **2012,** *46*, (5), 494-503.
42. C. R. Keenan, R. Goth-Goldstein, D. Lucas, D. L. Sedlak, Oxidative Stress Induced by Zero-Valent Iron Nanoparticles and Fe(II) in Human Bronchial Epithelial Cells, EST, 2009, 43, 4555-4560.
43. A. Thit, H. Selck, H. F. Bjerregaard, Toxicity of CuO nanoparticles and Cu ions to tight epithelial cells from Xenopus laevis (A6): Effects on proliferation, cell cycle progression and cell death, Toxicology in Vitro, 2013, 27, 1596-1601.
44. B. Fahmy, S. A. Cormier, Copper oxide nanoparticles induce oxidative stress and cytotoxicity in airway epithelial cells, Toxicology in Vitro, 2009, 23, 1365-1371.
45. El-Gendy, N.; Desai, V.; Berkland, C., Agglomerates of ciprofloxacin nanoparticles yield fine dry powder aerosols. *Journal of Pharmaceutical Innovation* **2010,** *5*, (3), 79-87.
46. Veghte, D. P.; Altaf, M. B.; Haines, J. D.; Freedman, M. A., Optical properties of non-absorbing mineral dust components and mixtures. *Aerosol Science and Technology* **2016,** *50*, (11), 1239-1252.
47. Pal, S.; Tak, Y. K.; Song, J. M., Does the Antibacterial Activity of Silver Nanoparticles Depend on the Shape of the Nanoparticle? A Study of the Gram-Negative Bacterium Escherichia coli. *Applied and Environmental Microbiology* **2007,** *73*, (6), 1712-1720.

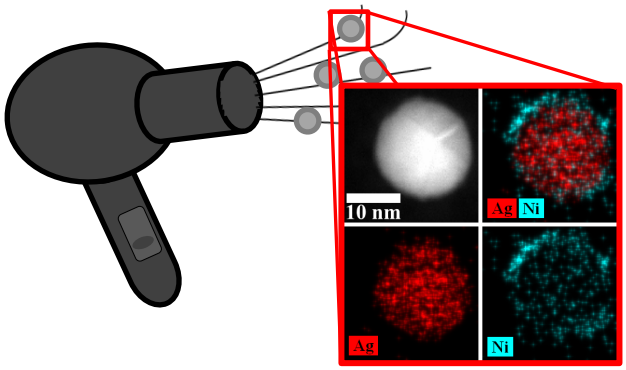


**Figure 0:** For TOC use only